

Aeolian erosion of storage piles yards: contribution of the surrounding areas

B. Furieri · J. M. Santos · S. Russeil · J.-L. Harion

Received: 31 July 2012 / Accepted: 23 May 2013 / Published online: 19 June 2013
© Springer Science+Business Media Dordrecht 2013

Abstract Dust emissions from stockpiles surfaces are often estimated applying mathematical models such as the widely used model proposed by the USEPA. It employs specific emission factors, which are based on the fluid flow patterns over the near surface. But, some of the emitted dust particles settle downstream the pile and can usually be re-emitted which creates a secondary source. The emission from the ground surface around a pile is actually not accounted for by the USEPA model but the method, based on the wind exposure and a reconstruction from different sources defined by the same wind exposure, is relevant. This work aims to quantify the contribution of dust re-emission from the areas surrounding the piles in the total emission of an open storage yard. Three angles of incidence of the incoming wind flow are investigated (30°, 60° and 90°). Results of friction velocity from numerical modelling of fluid dynamics were used in the USEPA model to determine dust emission. It was found that as the wind velocity increases, the contribution of particles re-emission from the ground area around the pile in the total emission also increases. The dust emission from the pile surface is higher for piles oriented 30° to the wind direction. On the other hand, considering the ground area around the pile, the 60° configuration is responsible for higher emission rates (up to 67 %). The global emissions assumed a minimum value for the piles oriented perpendicular to the wind direction for all wind velocity investigated.

Keywords Re-emission of settled dust · Dust emission quantification · USEPA model · CFD

B. Furieri (✉) · S. Russeil · J.-L. Harion
Mines Douai, EI, 59500 Douai, France
e-mail: bruno.furieri@mines-douai.fr

B. Furieri · S. Russeil · J.-L. Harion
Univ Lille Nord de France, 59000 Lille, France

J. M. Santos
DEA, Universidade Federal do Espírito Santo, Vitoria ES, 29060-970, Brazil

1 Introduction

Diffuse sources such as open storage yards are commonly found at industrial sites. Aeolian erosion of granular material may cause release of large quantities of dust to the atmosphere. The dust emitted may present a wide range of particle size fractions: lower than $2.5\mu\text{m}$, lower than $10\mu\text{m}$ or coarse particles up to $30\mu\text{m}$. The several particle size fractions have different effects on human health, mainly respiratory and cardiovascular risks. The estimation of dust emission from stockpiles is often carried out by two approaches: field measurements or mathematical models. The most widely used mathematical model to estimate dust emissions from stockpiles is that proposed by the United States Environmental Protection Agency (USEPA) [13]. This is an empirical model based on several experimental measurements that defines an emission factor which relates the average emission rate to an independent variable (for example, source mass or dimensions, production rate or number of sources). The emission factor used to estimate dust emission rates from stockpiles depends on the erosion potential which is a function of the friction velocity on the stockpile surface and the threshold friction velocity u_t^* (defined as the friction velocity above which particles take off). The USEPA model proposes a subdivision of the whole pile surface area into isosurfaces of the friction velocity. Each of these areas is treated as a distinctive source and the total dust emission is afterward calculated as a summation of the emissions from each area. The variety of particle size fractions is not an object of study in the USEPA model quantification.

A literature review shows several works using the USEPA model to quantify dust emission rates from storage piles [1–3, 7, 8, 10, 11]. Badr and Harion [1] investigated the influence of wind flow conditions and pile dimensions (height and width) on dust emission rates of an aggregate storage pile using the USEPA model. Numerical simulations were carried out to obtain the needed local wind properties near the pile. The authors concluded that changing pile configuration can reduce dust emissions. It was also found that an intermediate pile height shape leads to lower dust emissions, reaching 24 % of reduction from their maximum values. Toraño et al. [7] also carried out a similar study on various shapes of piles. These authors found a strong influence of the wind flow on the typical fluid flow structures around a pile and consequently on the dust emission rates calculated by using the USEPA model. Toraño et al. [7] also stated that a semicircular stockpile shape corresponds to lower emission rate when compared to conic and flat-topped stockpile shapes. Diego et al. [2] carried out an implementation of the USEPA model in a commercial CFD package to calculate emission rates. They investigated a configuration of parallel stockpiles and found out that one pile works as a protection to the other pile. Toraño et al. [8] studied the influence of wind barriers on dust emissions from storage piles using numerical simulation and the USEPA model and compared their results with literature data and industrial measurements. Their study has shown a reduction of about 66 % on dust emission due to the existence of barriers. Turpin and Harion [10] based their work on the analysis of the great influence of the stockpile crest on the overall dust emission. Several clipping heights of flat-topped piles were examined to determine their impact on dust emission. The main conclusion was that the flattening of stockpile's crest does not reduce the pollution. Turpin and Harion [11] employed the USEPA model to investigate the influence of nearby buildings on dust emissions from stockpiles of real industrial sites. The complex configuration of these sites was simulated: three stockpiles and several rectangular and cylindrical buildings. The remarkable influence of the obstacles on the total stockpile dust emissions was highlighted by these results. Ferreira et al. [3] performed numerical and experimental simulations of fluid flow around a conical pile under atmospheric flow conditions influenced by wind barriers. Although these authors have not quantified dust emissions, they compared the u_s/u_r distribution to experimental results of pile erosion and a consistent correlation was observed.

The studies described above used different techniques to investigate the influence of various parameters on the emission rate. However, it is worth noting that, these works did not take into account the emissions from the ground surface around the stockpiles. In industrial sites, the vicinity of a stockpile is significantly loaded with small granular particles originated from: piles perturbations, pile erosion or transport of material in the surrounding regions. Furieri et al. [5] have previously studied the near wall flow features (by the oil-film flow visualization technique) and three-dimensional air flow structure around piles (using numerical simulations validated by PIV measurements). The presence of regions of potential particles take-off from the ground was highlighted by the authors.

The present work aims to quantify the amount of particles emitted from the stockpile and from the ground surface around the pile. The friction velocity distribution on the pile surface and on the ground around the pile is calculated by using CFD. The USEPA model, usually employed to quantify the amount of particles from the stockpile, is used here to quantify emissions from the surrounding ground region. The contribution of particles re-emission from the ground around a pile in the overall dust emission from an open storage yard is discussed considering three different stockpiles orientations and its dependence on wind velocity magnitude.

2 Numerical simulation background

Numerical simulations were performed to solve the three-dimensional Reynolds Averaged Navier-Stokes equations governing the flow around the stockpile using a finite volume based CFD code [4]. Figure 1 shows the computational domain and the boundary conditions. The dimensions of the real stockpile (115.6 m (width), 41 m (length) and 16 m (height)) were scaled-down by a factor of 1:200 for numerical simulations: 0.578 m (width), 0.205 m (length) and 0.08 m (height). The model tested was an oblong stockpile with an angle of repose equal to 38° [12] representative of coal piles commonly found in real industrial sites. Spanwise and vertical dimensions correspond to the wind-tunnel dimensions where PIV experiments were carried out to validate the results of numerical simulations, see Turpin [9]. Dimensions of upstream and downstream zones were chosen to ensure that the results are not influenced by the size of the domain. In fact, the vertical dimension of the computation domain was set as

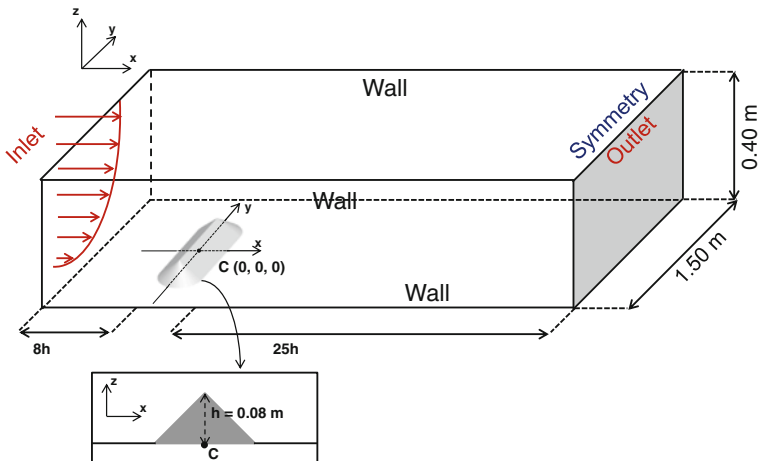


Fig. 1 Schematic configuration of the computational domain and boundary conditions

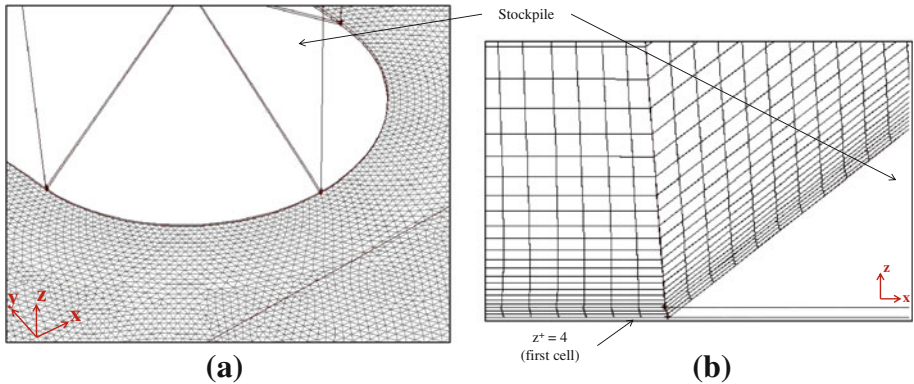


Fig. 2 Mesh **a** on the ground surface ($z = 0$) around the pile and **b** above the stockpile surface on the symmetry plane ($y = 0$)

half of the wind-tunnel height. Turbulence effects were accounted for by using the $k-\omega$ Shear Stress Transport (SST) model with the option Transitional Flow (available on the FLUENT package [4]). This option yields the enhancement of certain modelling conditions: adverse pressure gradient, flow separation and reattachment [10,9]. Mesh size was chosen based on sensitivity tests previously carried out by Badr and Harion [1] for the same configurations. The size of the first cell at the wall was taken as $z^+ = 4$ ($z^+ = \rho u^* z / \mu$), as required for the use of this turbulent model ($z^+ \leq 5$) to ensure that no wall functions are used (for better accuracy) to account for the turbulence damping near walls. The mesh is produced by an extrusion from triangular cells defined on the ground surface and pile walls (see Fig. 2a) towards the top boundary of the computational domain (see Fig. 2b).

The inlet boundary conditions for velocity (u , v and w), turbulent kinetic energy (k) and specific dissipation rate (ω) were obtained from previous numerical simulations of a flow in a channel with the same dimensions (height and width) of the computational domain used in the present work. In these previous simulations, a periodic streamwise flow was set to produce a fully developed channel flow and the converged flow field is considered to be the inlet condition for the present simulation. For the outlet boundary conditions, it is assumed that the flow is fully developed and for the upper boundary condition, symmetry was imposed. Finally, smooth walls with no-slip conditions are set at domain lateral walls, as well, at stockpile and ground walls. Further details of the numerical procedure can be found in Turpin [9].

3 USEPA model to estimate aeolian dust emission

This section presents two distinctive parts. At first, the USEPA mathematical model is described in details by an algorithm. Each parameter is also presented with the explanation of the chosen value in our study. The second part deals with the discretisation levels that are obtained when CFD simulations are used.

3.1 Mathematical model set-up

The model used for the assessment of dust emission [13] is presented herein under an algorithm chart in Fig. 3. Several input data are required: particle size multiplier (taken for the average particles size) (k), wind erosion threshold friction velocity (u_t^*), distribution of u_s/u_r

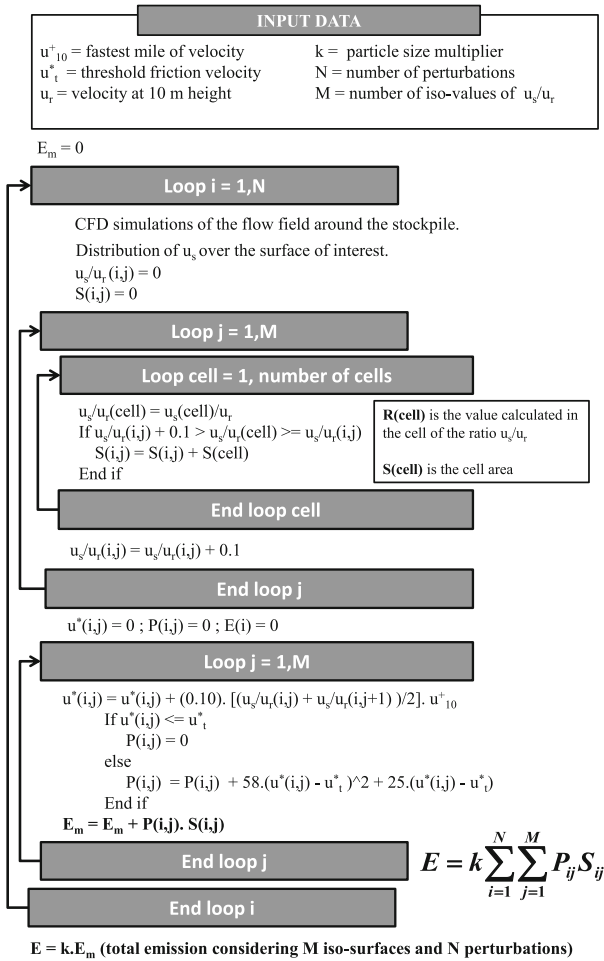


Fig. 3 USEPA model algorithm

on the surface of interest (u_r is the reference velocity at 10 m height from the ground and u_s is the velocity at 25 cm from the surface, both for real scale), number of perturbations (N), number of isosurfaces of u_s/u_r (M) and the highest velocity value (fastest mile wind speed) measured by an anemometer at a reference height for a period between perturbations (u^+_{10}).

A perturbation is defined in the USEPA guide [13] as an intervention done on a storage pile yard for maintenance and transport of material. The first loop concerns the number of perturbation per year (operations on pile’s surfaces). For the sake of simplification, the results of dust emission in the present work are presented in kg per perturbation. The number of perturbations should be defined for a practical application of emission quantification on a real industrial site.

It is worth noting that, the u_s/u_r ratios which are obtained by CFD calculations are strongly influenced by the wind flow direction, which changes during a day in industrial sites. The threshold friction velocity value is subjected to particle matter characteristics, such as granulometry, density, moisture and, if existent, surface treatment. The friction velocity is calculated based on the ratio between near wall velocity u_s and free stream velocity u_r .

The USEPA model is based on emission factors, see Eq. 1. The methodology consists in implementing Eq. 1 to calculate the emission rate (E). The whole pile surface is divided in different subareas each representing a given level of wind erosion exposure, i. e., a value of the ratio u_s/u_r . Each subarea is then considered as a single source (this explains the summation in Eq. 1).

$$E = k \sum_{i=1}^N \sum_{j=1}^M P_{ij} S_{ij} \quad (1)$$

where P_{ij} is the erosion potential (g/m^2) and $S_{ij}(\text{m}^2)$ is the fraction of the surface area (subarea) corresponding to a constant value of u_s/u_r . In this equation, the erosion potential is calculated based on the difference between the friction velocity (u^*) for the fastest mile of the wind and the wind erosion threshold friction velocity (u_t^*) as shown in Eq. 2.

$$\begin{cases} P = 58 (u^* - u_t^*)^2 + 25 (u^* - u_t^*) & \text{for } u^* > u_t^* \\ P = 0 & \text{for } u^* \leq u_t^* \end{cases} \quad (2)$$

The friction velocity is then calculated as presented in Eq. 3 which is based on the logarithmic velocity profile of the undisturbed surface boundary layer. However, for the fluid flow disturbed by a stockpile the USEPA model proposes Eq. 4 to determine friction velocity.

$$u^* = 0.053 u_{10}^+ \quad (3)$$

$$u^* = 0.10 \left(\frac{u_s}{u_r} \right) u_{10}^+ \quad (4)$$

Figure 4a shows an example of typical contours of u_s/u_r calculated by numerical simulations. From the calculation of the friction velocity we can define erodible and non-erodible zones over the surfaces of interest. Zones with friction velocity greater than the erosion threshold value are denominated erodible. On the other hand, for $u^* < u_t^*$, zones are called non-erodible. Larger values of u_s/u_r are found downstream the stockpile. Wall shear stress and friction velocity values are also large. On the other hand, in the stagnation zone, upstream the pile, the lowest levels of u_s/u_r are noticed. Finally, the dashed ellipses presented in Fig. 4a are examples of areas over the ground surface in which the surface boundary layer is not disturbed by the stockpile. It can be checked by the values of u_s/u_r on these regions. Indeed, from the logarithmic law governing an undisturbed wind velocity profile [6] for a roughness height equal to 0.03 m (open flat terrain) [14] the value of u_s/u_r over an undisturbed region is approximately 0.366 (see Fig. 6). This value is identical to that found in the numerical simulation (highlighted in the colormap of u_s/u_r values in Fig. 4a).

In order to calculate the re-emission of silt particles settled on the ground surface around the stockpile, two input parameters of the formulations presented above (Eqs. 1–4) have different values to that usually used to assess the emissions from the stockpile surface.

Firstly, a delimited surface S must be defined around the pile to represent the region in which the amount of settled dust has to be assessed. The choice of the dimensions of this area should be driven by the quantity of material emitted by the stockpile surface and on how far it accumulates or other source such as material transport and pile maintenance and can be determined by field observations in industrial sites. The dimensions of the surface S were defined arbitrarily by the authors as about ten times the stockpile surface area (Fig. 5). Figure 5 then presents the two characteristic regions: (i) the stockpile vicinity is the surface taken into account to calculate the re-emission and (ii) the zone far away from the stockpile where the ratio u_s/u_r is approximately equal to 0.366 (undisturbed velocity profiles).

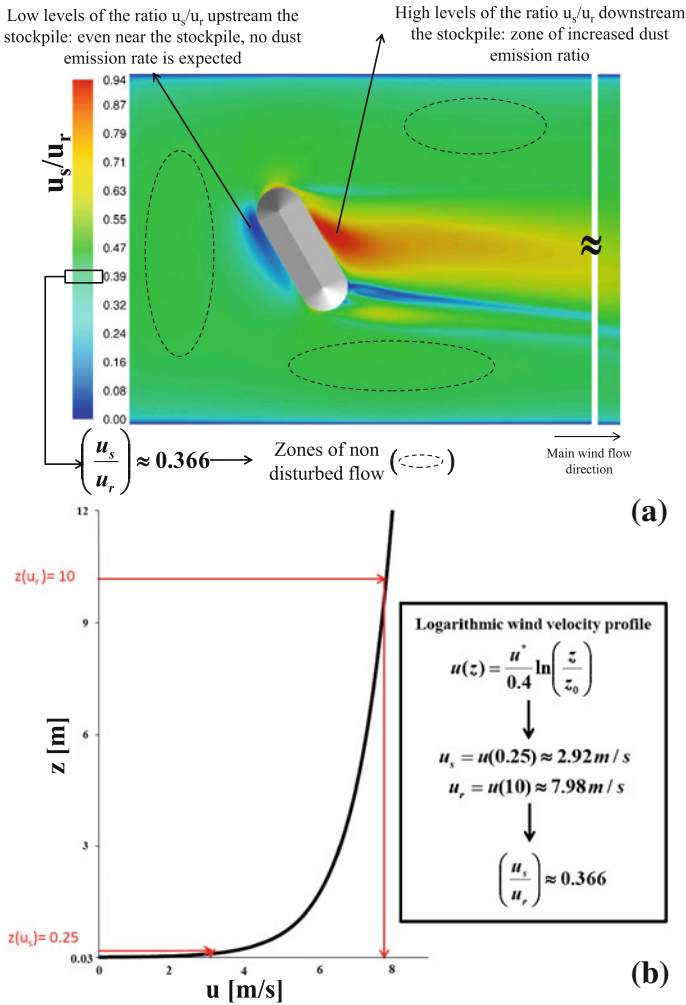


Fig. 4 **a** Typical contours of u_s/u_r on the horizontal plane parallel at 0.25 m above the ground surface (it corresponds to 0.00125 in the wind-tunnel and numerical scale). **b** Vertical logarithmic profile of wind velocity [6] that is used to calculate u_s/u_r in the undisturbed flow zones.

The second parameter to be chosen is the erosion threshold friction velocity for the surrounding regions. The USEPA guide gives values of u_t^* for several materials and conditions and among them the value for the ground surrounding a stockpile (cf. Table 13.2.5–2 in US-EPA [13]). For coal on the ground surface around the pile a value of 0.55 m/s is proposed. It can be compared to the value of 0.35 m/s that was used in the calculation of dust emission from the stockpile surface. The value for the stockpile surface was determined from wind-tunnel experiments (cf. Turpin and Harion [10]).

The other input values, aerodynamic particle size multiplier (k) and fastest mile of the wind velocity (u_{10}^+), remain unchanged and are equally used in both quantifications on and around the stockpile. The aerodynamic particle size multiplier (k), as indicated by the USEPA model, assumes a value for each aerodynamic particle size (cf. Sect. 13.2.5.3 in USEPA [13]). The value of k equal to 0.5 was chosen to represent PM_{10} emissions.

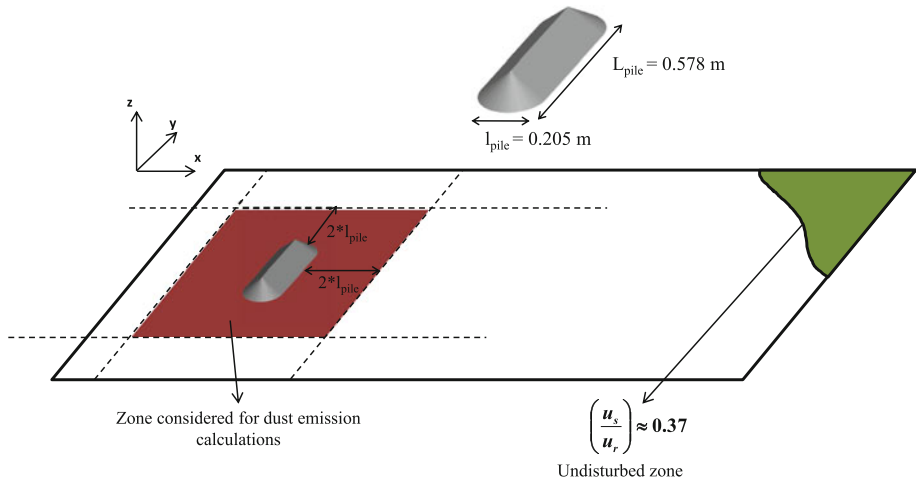


Fig. 5 Schematic representation of undisturbed zone away from the pile and zone considered for dust emission calculations including the stockpile and the ground surface where re-emission of settled particles may occurs (for perpendicular configuration)

Three values of the fastest mile of the wind velocity (u_{10-A}^+ , u_{10-B}^+ and u_{10-C}^+) were chosen to represent different situations of dust re-emission:

- no dust emission at all (u_{10-A}^+),
- dust emission over the whole region (u_{10-B}^+),
- no dust emission over the undisturbed area (surface boundary layer) and emission from the region disturbed by the stockpile (u_{10-C}^+).

For the third case (u_{10-C}^+), the wind erosion friction velocity has to be chosen lower than the erosion threshold velocity around the piles, i. e., $u^* \leq 0.55$ m/s. Then considering Eq. 3 which links the friction velocity and the fastest mile wind velocity, the value of u_{10}^+ can be defined:

$$u_{10}^+ \leq 10.38 \text{ m/s} \quad (5)$$

Finally, a smaller and a greater value than $u_{10-C}^+ = 10.38$ m/s were chosen to represent the two other cases above mentioned: $u_{10-A}^+ = 5.0$ and $u_{10-B}^+ = 15.0$ m/s.

3.2 Dust emission estimation using different subarea discretisation levels

The original USEPA model proposes a distribution of the u_s/u_r ratio for stockpiles based on wind-tunnel measurements (Fig. 6). Previous numerical studies (cf. Badr and Harion [1] and Toraño et al. [7]) were carried out to investigate the u_s/u_r distribution on the pile surface. However, the USEPA model proposes a maximum of four subareas of u_s/u_r , mainly due to the feeble velocity distribution detail obtained by the wind-tunnel experiments in which the model is based on. Contrarily, the CFD technique yields to a detailed velocity distribution and thus it is possible to enlarge the number of subareas used in the emission model. For example, Badr and Harion [1] and Turpin and Harion [10] presented seventeen subareas for oblong stockpiles obtained by CFD presented in Fig. 7 (also, see Table 1). By comparing Figs. 6 and 7, it can be seen that the distribution of u_s/u_r is quite similar in both cases, although the

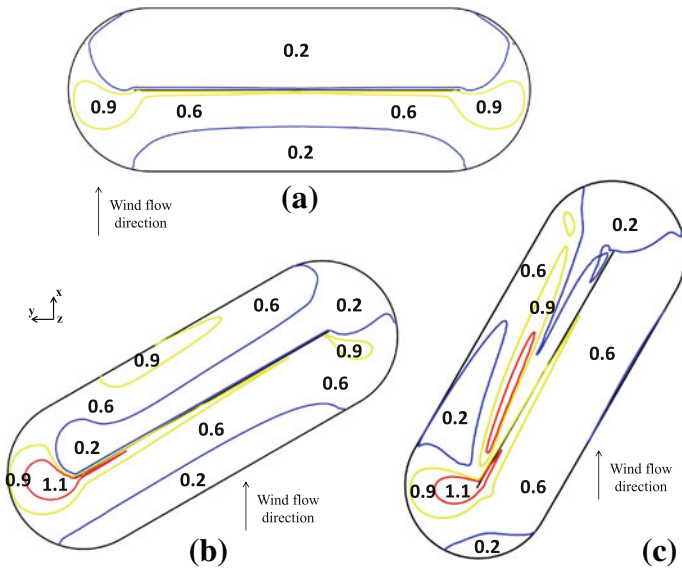


Fig. 6 Subdivision of the stockpile surface in four subareas corresponding to constant values of u_s/u_r as proposed by the USEPA for **a** perpendicular, **b** 60° and **c** 30° configurations

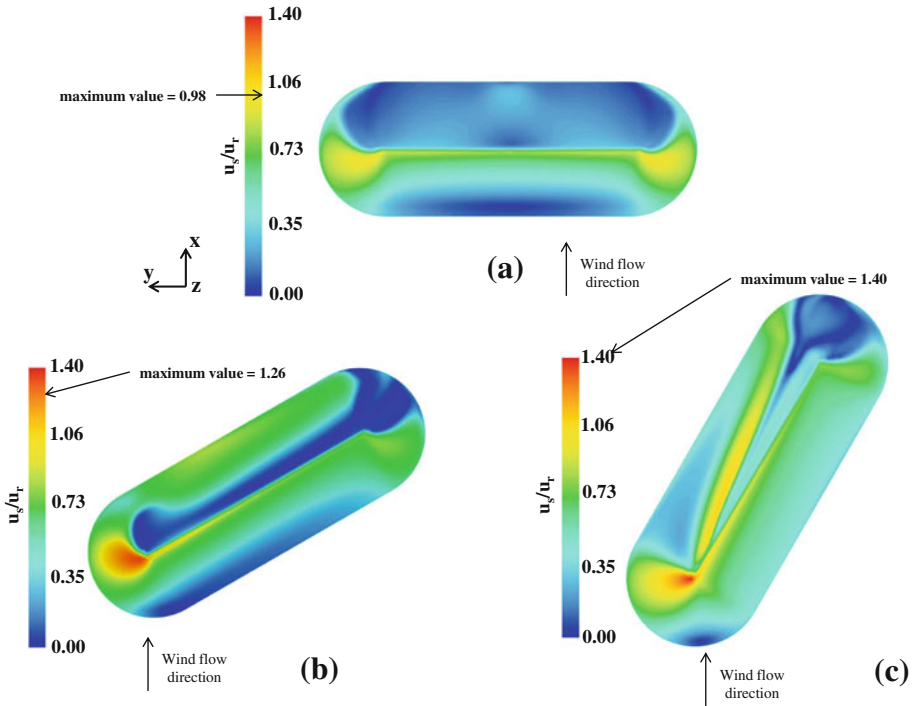


Fig. 7 Contours of u_s/u_r on the planes parallel to the stockpile surface at 0.25 m above the pile surface in real scale (it corresponds to 0.00125 in the wind-tunnel and numerical scale) for **a** perpendicular, **b** 60° and **c** 30° configurations

Table 1 Chosen values of u_s/u_r to be replaced in the equations of the USEPA methodology of dust quantification: in left of the table those originally proposed by the model and in right those taken from numerical simulations

USEPA model [13]		Reference works	
u_s/u_r range	Chosen value	u_s/u_r range	Chosen value
$0.0 \leq u_s/u_r < 0.4$	0.20	$0.0 \leq u_s/u_r < 0.1$	0.05
		$0.1 \leq u_s/u_r < 0.2$	0.15
		$0.2 \leq u_s/u_r < 0.3$	0.25
		$0.3 \leq u_s/u_r < 0.4$	0.35
$0.4 \leq u_s/u_r < 0.8$	0.60	$0.4 \leq u_s/u_r < 0.5$	0.45
		$0.5 \leq u_s/u_r < 0.6$	0.55
		$0.6 \leq u_s/u_r < 0.7$	0.65
		$0.7 \leq u_s/u_r < 0.8$	0.75
$0.8 \leq u_s/u_r < 1.0$	0.90	$0.8 \leq u_s/u_r < 0.9$	0.85
		$0.9 \leq u_s/u_r < 1.0$	0.95
$u_s/u_r \geq 1.0$	1.10	$1.0 \leq u_s/u_r < 1.1$	1.05
		$1.1 \leq u_s/u_r < 1.2$	1.15
		$1.2 \leq u_s/u_r < 1.3$	1.25
		$1.3 \leq u_s/u_r < 1.4$	1.35
		$1.4 \leq u_s/u_r < 1.5$	1.45
		$1.5 \leq u_s/u_r < 1.6$	1.55
		$1.6 \leq u_s/u_r < 1.7$	1.65

Reference works Badr and Harion [1] and Turpin and Harion [10]

Table 2 Dust emission estimation for two different discretisation levels of u_s/u_r distribution

u_{10}^+ m/s	Wind angle of incidence	Emission (kg/perturbation)		Difference (%)
		USEPA [13]	Reference works	
5.00	90°	0.7	0.8	7.4
	60°	1.4	1.5	9.2
	30°	1.4	1.6	11.2
10.38	90°	16.5	16.5	0.0
	60°	29.1	30.0	3.2
	30°	33.2	32.6	-1.7
15.00	90°	43.1	44.4	3.0
	60°	76.1	79.7	4.8
	30°	87.4	87.5	0.1

Reference works Badr and Harion [1] and Turpin and Harion [10]

maximum values of u_s/u_r are slightly different and, furthermore, these differences increase as the stockpile orientation becomes aligned to the wind direction.

Table 2 synthesizes a comparison between dust emission quantification using these different discretisation levels. Although, both methods indicate an increment in dust emission from the perpendicular configuration to the stockpile oriented 30°, the more refined discretisation applied by Badr and Harion [1] and Turpin and Harion [10] permits better interpretation of the stockpile wind exposure. The maximum difference found was approximately 11.2 % and most cases showed differences reaching a maximum value of 5 %. These differences are more pronounced for $u_{10}^+ = 5.0$ m/s. The results obtained by using the USEPA discretisation method may underestimate dust emission due to the fact that the USEPA model also underestimates the maximum values of u_s/u_r on the piles surface.

4 Results

4.1 Wind exposure of pile surface

Figure 7 presents the distribution of u_s/u_r on the three piles' surfaces and features the influence of main wind direction. The scale of u_s/u_r values in the figure is the same for all orientations allowing a better visualization of the differences. In Fig. 7a, the stockpile is perpendicular to the wind direction and the maximum value of u_s/u_r is 0.98 which is the lowest among all investigated configurations. The highest levels of u_s/u_r are located on the pile crest and on both pile sides. In these regions, the flow is accelerated and detaches from the stockpile (Turpin and Harion [10]). The ratio u_s/u_r progressively increases with height on the windward wall. The minimum values of u_s/u_r are found on the leeward wall in the zone of recirculating flow.

The modification in the stockpile orientation deeply changes the u_s/u_r distribution, as is noticed in Fig. 7b, c. The u_s/u_r distribution patterns for the 60° configuration (Fig. 7b) shows that the highest levels of u_s/u_r are found on the left side of the windward wall (maximum value equal to 1.26) where an helical vortex arises and causes velocity augmentation (Turpin and Harion [10] and Furieri et al. [5]). In this configuration, the helical vortex is also responsible for the high values of u_s/u_r on the leeward wall. The configuration 30° presents almost the same flow pattern as noticed for 60° except for some details downstream. The u_s/u_r distribution pattern for the 30° configuration (Fig. 7c) shows that the maximum values of the u_s/u_r are found on the pile crest and windward wall where large part of the surface exhibits values of u_s/u_r greater than 0.70 whereas for the perpendicular configuration it displays values between 0.10 and 0.50 and for the 60° configuration these values are in the range between 0.40 and 0.80.

4.2 Wind exposure of ground surface around a pile

Figures 8a, 9a and 10a present u_s/u_r distribution on the ground around the stockpile for the whole domain. The zone near the stockpile considered in dust emission calculations (as defined in Fig. 5) is highlighted by means of dashed lines. Figures 8b, 9b and 10b present the zones where friction velocity (u^*) is larger than the threshold friction velocity for the ground region ($u_t^* = 0.55$ m/s) for a situation in which u_{10}^+ is equal to 10.38. These figures highlight only the contours of u_s/u_r larger than 0.50. From Eq. 4, u_s/u_r values larger than 0.50 indicate a friction velocity larger than 0.57 m/s. Indeed, according to Eq. 2, an emission event occurs as the friction velocity of the considered subarea is higher than 0.55 m/s which is the case for the highlighted regions. Finally, Figs. 8c, 9c and 10c represent the fluid flow streamlines over the stockpiles coloured by the streamwise component of the vorticity.

For the perpendicular configuration, the dust emission zones are located on both stockpile lateral sides as shown in Fig. 8. These are flow acceleration zones (Turpin and Harion [10] and Furieri et al. [5]) where the flow structures formed due to the stockpile presence cause high levels of friction velocity and, consequently, particles take-off events. In the zone upstream the stockpile, as well as in the wake region, the friction velocity levels are lower and do not suggest the re-emission of settled dust. Figure 8c shows main vortices developing. These vortices have opposite values of the X-vorticity meaning that they are contra-rotative. Moreover, the contours of the zones suggesting dust re-emission (Fig. 8b) indicate downstream the pile the downwash effects (fluid flow impinging vertically the ground causing high velocity gradient values) on the wall of these contra-rotative vortices. The lateral sides of each main vortex

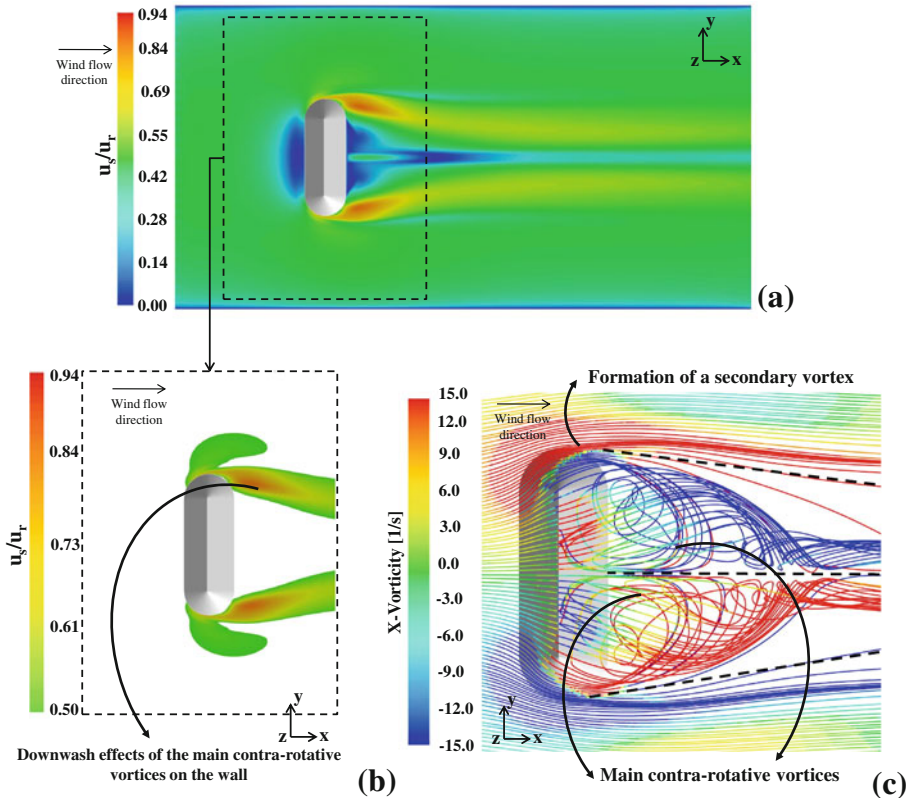


Fig. 8 Contours of u_s/u_r on the horizontal plane parallel at 0.25 m above the ground surface in real scale (it corresponds to 0.00125 in the wind-tunnel and numerical scale) for perpendicular configuration: **a** on the whole ground surface and **b** on the ground surface considered for dust emission calculations. **c** Streamlines coloured by the X-vorticity

also present a secondary vortex, which is smaller and contra-rotative to the main vortex. The zones of formation of the secondary vortex are the flow acceleration.

Figures 9a, b show the u_s/u_r distribution on the ground for the 60° configuration. The region of dust emission, in which the friction velocity is greater than the threshold friction velocity, is larger for this configuration. The main vortex formed downstream the pile and the intense velocity gradients near wall in this region downstream the pile (Turpin and Harion [10] and Furieri et al. [5]) is the flow structure responsible for the high values of u_s/u_r that cause high wall shear stress. Figure 9c show the single main vortex formed in this configuration. Also, in Fig. 9c, it is worth noting the secondary vortex with opposite values of X-vorticity which characterizes it as contra-rotative to the main vortex. Furthermore, the secondary vortex is responsible for a smaller zone of dust emission, highlighted in Fig. 9b.

Finally, Fig. 10a, b present the u_s/u_r distribution on the ground around the stockpile for the 30° configuration. Approximately, the values of u_s/u_r are in the range between 0.6 and 0.7, i.e. lower than those for the two other configurations investigated. In this orientation, as it was observed for 60°, there is a main vortex formed downstream the pile responsible for the zones of potential dust emissions. Figure 10c shows the streamlines of this structure. The main vortex in this configuration is smaller and present lower effects on the ground than the one formed in the configuration 60°.

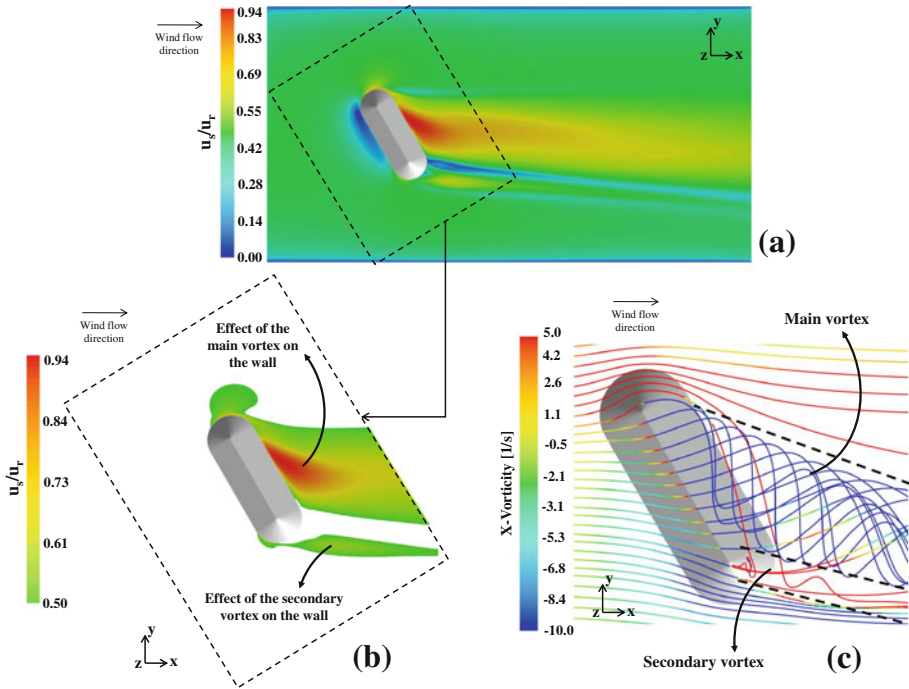


Fig. 9 Contours of u_s/u_r on the horizontal plane parallel at 0.25 m above the ground surface in real scale (it corresponds to 0.00125 in the wind-tunnel and numerical scale) for 60° configuration: **a** on the whole ground surface and **b** on the ground surface considered for dust emission calculations. **c** Streamlines coloured by the X-vorticity

For all wind flow orientations, details about wall shear stress distribution, vortices, down-wash and upwash zones are shown in the work of Furieri et al. [5].

4.3 Quantitative analysis of dust emissions

This section presents the results obtained by using the USEPA model previous presented in Sect. 3. Table 3 presents the percentage of erodible and non-erodible areas on and around the stockpile (based on the total area of the considered surface, see Fig. 5) that are calculated by summation of subareas for each u_s/u_r range (see Eq. 1). The friction velocity was calculated using u_{10}^+ equal to 10.38 m/s as presented in Eq. 5. The erodible area on the stockpile was found larger for the 30° configuration than for the other configurations, reaching about two times the value calculated for the perpendicular configuration. The results in Table 3 showed that the erodible area around the stockpile, for all configurations, is smaller than the erodible area on the stockpile surface. It can be explained by the fact that the threshold friction velocity is higher for the region around the stockpile and the ratio of u_s/u_r is higher on the stockpile surface. Thus, for the perpendicular configuration, the percentage of erodible area is equal to 42.1 % on the stockpile and 16.9 % around the pile. For the 60° and 30° configurations, respectively, these values are 72.4 and 26.5, and 84.4 and 19.7 %. In addition, the results presented in Table 3 shows that the highest percentage of erodible area on pile surface was found for the 30° configuration and around the pile the same trend was found for the 60° configuration. This large erodible area around the stockpile for the 60° configuration may

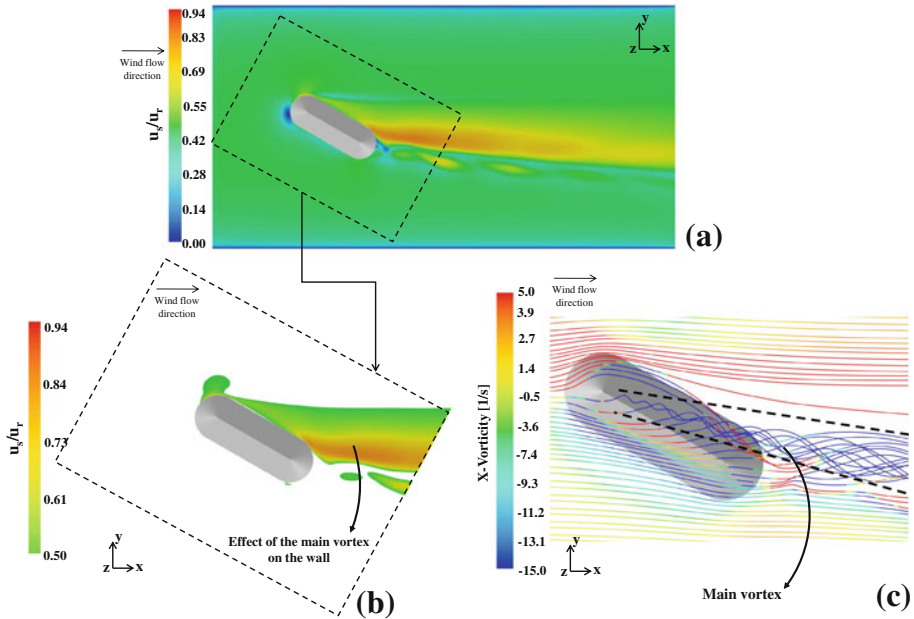


Fig. 10 Contours of u_s/u_r on the horizontal plane parallel at 0.25 m above the ground surface in real scale (it corresponds to 0.00125 in the wind-tunnel and numerical scale) for 30° configuration: **a** on the whole ground surface and **b** on the ground surface considered for dust emission calculations **c** Streamlines coloured by the X-vorticity

be explained by the intense and larger main vortex formed downstream the pile close to the leeward wall and extended to the far wake region.

Table 4 synthesizes the overall data of dust emission estimation from stockpile surface and ground surface around the pile. The emission rates are calculated for different values of u_{10}^+ . For all the values of u_{10}^+ investigated, the stockpile emissions are higher for the 30°. For instance, if $u_{10}^+ = 10.38$, in this configuration the emission per perturbation is equal to 32.6 kg whereas for the 60° and 90° configurations it was found equal to 30.0 and 16.5 kg, respectively. The ground surface surrounding the pile gives the highest values of dust emissions for the 60° configuration (22.6 kg for $u_{10}^+ = 10.38$) while the other configurations it gives smaller values of dust emissions per perturbation (7.9 kg for 90° configuration and 12.8 kg for 30° configuration for the same fastest mile of the wind velocity). Table 4 illustrates the importance of re-emission by showing that the existence of silt particles on the ground around the pile and their emission due to the wind erosion cannot be neglected. For u_{10}^+ equal to 10.38 m/s, the contribution of re-emission is approximately 30 % for the 90° and 30° configurations and reaches about 43 % for the 60° configuration. For u_{10}^+ equal to 15 m/s, the contribution of re-emission doubles while for u_{10}^+ equal to 5 m/s, the re-emission is found to be negligible.

5 Conclusions

A quantitative investigation of particles re-emission from the regions surrounding stockpiles by using the USEPA methodology was presented. In order to estimate emissions rates from

Table 3 Erodible and non-erodible areas for $u_{10}^+ = 10.38$ m/s on ($u_t^* = 0.35$ m/s) and around ($u_t^* = 0.55$ m/s) the stockpile

u_s/u_r	u (m/s)	%			u_s/u_r	u (m/s)	%		
		On the stockpile					Around the stockpile		
		90°	60°	30°			90°	60°	30°
0.05	0.05	9.5	6.0	2.7	0.05	0.05	3.2	0.4	0.1
0.15	0.16	28.2	11.7	5.6	0.15	0.16	5.7	2.9	0.4
0.25	0.26	20.2	9.9	7.3	0.25	0.26	7.5	3.7	1.5
	Non-erodible	57.9	27.6	15.6	0.35	0.36	13.8	14.7	17.8
0.35	0.36	6.7	9.8	9.7	0.45	0.47	52.9	51.8	60.5
0.45	0.47	7.1	11.1	15.9		Non-erodible	83.1	73.5	80.3
0.55	0.57	7.4	13.0	20.3	0.55	0.57	8.6	10.5	10.1
0.65	0.67	6.7	13.9	15.3	0.65	0.66	6.5	11.2	5.8
0.75	0.78	5.9	12.2	10.9	0.75	0.77	1.8	3.4	3.8
0.85	0.88	5.4	7.5	5.4	0.85	0.88	0.0	1.4	0.0
0.95	0.99	2.9	2.3	3.5	0.95	0.99	0.0	0.0	0.0
1.05	1.09	0.0	1.4	2.4	1.05	1.10	0.0	0.0	0.0
1.15	1.19	0.0	0.9	0.6	1.15	1.21	0.0	0.0	0.0
1.25	1.30	0.0	0.3	0.3	1.25	1.32	0.0	0.0	0.0
1.35	1.40	0.0	0.0	0.1	1.35	1.43	0.0	0.0	0.0
1.45	1.50	0.0	0.0	0.0	1.45	1.54	0.0	0.0	0.0
1.55	1.61	0.0	0.0	0.0	1.55	1.65	0.0	0.0	0.0
1.65	1.71	0.0	0.0	0.0	1.65	1.76	0.0	0.0	0.0
	Erodible	42.1	72.4	84.4		Erodible	16.9	26.5	19.7

Values in bold represent an accumulation of surface percentage

Table 4 Dust emissions from stockpile surface and ground surface around the pile

		Emissions (kg/perturbation)			Contribution (%)		
			u_{10}^+ (m/s)			u_{10}^+ (m/s)	
			5	10.38		15	5
On the pile	90°	0.8	16.5	44.4	100	67.7	34.2
	60°	1.5	30.0	79.7	100	57.1	32.8
	30°	1.6	32.6	87.5	100	71.8	41.1
Surrounding the pile	90°	0.0	7.9	85.2	0.0	32.3	65.8
	60°	0.0	22.6	163.5	0.0	42.9	67.2
	30°	0.0	12.8	125.6	0.0	28.2	58.9
Global emissions	90°	0.8	24.4	129.6			
	60°	1.5	52.6	243.2			
	30°	1.6	45.4	214.1			

the ground surface around the stockpile, some input parameters have specific values to fit the conditions of this region: threshold friction velocity and the dimensions of the region where the re-emission may occur. The influence of the fastest mile of the reference velocity and pile orientation in relation to wind direction were investigated.

The value of k equal to 0.5 was chosen to represent PM_{10} emissions from both regions analysed. The threshold friction velocity equal to 0.55 m/s was applied for particles take-off from the ground surface around the pile and 0.35 m/s for emissions from the stockpile surface. The fastest mile of the reference velocity equal to 10.38 m/s was taken as the limit value for which there is no emission from the undisturbed region in the vicinity of the stockpile. Under these conditions the ground surface where re-emission can occur is delimited by u_s/u_r greater than 0.50.

The present investigation shows that (i) there exists a zone of particles take-off downstream the pile and its size depends on the incoming wind flow direction and (ii) the contribution of re-emission of dust particles settled around in global emissions is significant.

It was established that as the wind velocity increases, the contribution of re-emission also increases. In fact, among the wind velocities tested, for values lower than 5 m/s, no contribution of re-emission in the global emission was found. The dust emission from the pile surface is larger for 30° configuration. On the other hand, considering the ground surface around the pile, the 60° configuration is responsible for a greater emission rate. The contribution of the re-emission in the global emissions has indicated a maximum value of 43 % for the 60° configuration for $u_{10}^+ = 10.38$ m/s. It can be concluded that for u_{10}^+ equal or greater than 10.38 m/s, re-emission from the ground surface around the pile must not be neglected or, as a consequence, the global emission from an open stockpile yard will be underestimated. Finally, the global emissions assumed a minimum value for the piles oriented perpendicular to the wind direction for all wind velocity investigated.

Acknowledgements This work was carried out with the financial support of EDF R&D.

References

1. Badr T, Harion J-L (2007) Effect of aggregate storage piles configuration on dust emissions. *Atmospheric Environ* 41:360–368
2. Diego I, Pelegry A, Torno S, Toraño J, Menendez M (2009) Simultaneous CFD evaluation of wind flow and dust emission in open storage piles. *Appl Math Model* 33:3197–3207
3. Ferreira A, Lambert R (2011) Numerical and wind tunnel modelling on the windbreak effectiveness to control the aeolian erosion of conical stockpiles. *Environ Fluid Mech* 11:61–76
4. FLUENT User's guide V6.3. <http://www.ansys.com/Products/Simulation+Technology/Fluid+Dynamics/ANSYS+Fluent>. Accessed Jan 2012
5. Furieri B, Russeil S, Harion J-L, Santos JM (2012) Experimental surface flow visualization and numerical investigation of flow structure around an oblong stockpile. *Environ Fluid Mech* 12(6):533–553
6. Hsu SA, Meindl EA, Gilhousen DB (1994) Determining the power-law wind-profile exponent under near-neutral stability conditions at sea. *J Appl Meteor* 33:757–765
7. Toraño J, Rodrigues R, Diego I, Rivas JM, Pelegry A (2007) Influence of the pile shape on wind erosion CFD emission simulation. *Appl Math Model* 31:2487–2502
8. Toraño J, Torno S, Diego I, Menendez M, Gent M (2009) Dust emissions calculations in open storage piles protected by means of barriers, CFD and experimental tests. *Environ Fluid Mech* 9:493–507
9. Turpin C (2010) Amélioration des modèles de quantification des émissions particulaires diffuses liées à l'érosion éolienne de tas de stockage de matières granulaires sur sites industriels. PhD Thesis, University of Valenciennes, Industrial Energy Department, Ecole de Mines de Douai
10. Turpin C, Harion J-L (2009) Numerical modelling of flow structures over various flat-topped stockpiles height: implications on dust emissions. *Atmospheric Environ* 43:5579–5587
11. Turpin C, Harion J-L (2010) Effect of the topography of an industrial site on dust emissions from open storage yards. *Environ Fluid Mech* 10:677–690
12. USEPA (1985) Windbreak effectiveness for storage-pile fugitive-dust control. A wind Tunnel Study. Department of Marine, Earth and Atmospheric Sciences, North Carolina State University, EPA, NC 27695–8208

13. USEPA (2006) Miscellaneous Sources, Industrial Wind Erosion, AP-42, 5th edn, vol I, Chap. 13.2.5, November 2006. <http://www.epa.gov/ttn/chieff/ap42/ch13/final/c13/final/c13s0205.pdf>. Accessed Jan 2012
14. World Meteorological Organization (2006) Guide to meteorological instruments and methods of observations, 7th edn. WMO, Geneva